JOURNAL OF GEOPHYSICAL RESEARCH, VOL. 94, NO. B4, PAGES 4441–4455, APRIL 10, 1989

A High-Resolution Seismic Reflection/Refraction Study of the Chugach-Peninsular Terrane Boundary, Southern Alaska

THOMAS M. BROCHER, MICHAEL A. FISHER, AND ERIC L. GEIST

U.S. Geological Survey, Menlo Park, California

NIKOLAS I. CHRISTENSEN

Department of Geosciences, Purdue University, West Lafayette, Indiana

We present results from a high-resolution seismic refraction analysis of the shallow (approximately 2 km) crustal structure along the 107-km-long Trans-Alaska Crustal Transect Chugach reflection line in southern Alaska and a comparison with laboratory measurements of field samples. The refraction analysis includes the two-dimensional interpretation of several thousand first- and secondary-arrival travel times digitized from 1024-channel split-spread common shot gathers. The velocity model derived from this analysis better defines the location and geometry of terrane boundaries than does the normal incidence reflection section and agrees well with surface mapping of lithologies. Furthermore, the model predicts travel times within 100 ms of the reflection times recorded from the base of the Quaternary on the Chugach reflection section. Thicknesses of Quaternary deposits, with velocities between 1.1 and 2.0 km/s, correlate inversely with the quantity of observed lower crustal reflections on the Chugach section, suggesting that the presence or absence of these sediments in sufficient thickness exerted primary control on the quality of the deeper portion of the section. There is a significant velocity contrast between crystalline rocks across the Border Ranges fault (5.0 versus 5.6 km/s), the major contact between the Chugach and Peninsular terranes, in agreement with laboratory measurements of field specimens. In the Peninsular terrane the modeling indicates that an unnamed fault delimiting the southern flank of the Copper River Basin dips steeply northward at 50° and has about 1300 m of vertical offset. Laboratory measurements document a maximum velocity anisotropy of 20% for phyllitic schists of the Valdez Group in the Chugach terrane. In agreement with the observed E-W strike and near-vertical dip of the Valdez Group, we determined a significant (14%) velocity anisotropy for ray paths oriented N-S versus NE-SW.

INTRODUCTION

Recent innovations in seismic data acquisition and in data processing and interpretation have blurred the formerly rigid distinctions between reflection and refraction profiling of the continental lithosphere. For example, the recording of densely sampled wave fields to ranges of 10 km and more during "reflection" experiments allows the precise definition of the velocity-depth structure of the upper 1–2 km of the crust. The analysis of refracted first arrivals recorded during reflection profiling has been used to examine the structure of the upper crust in the Rio Grande rift [*Jurdy and Brocher*, 1980; *Brocher*, 1981*a*], the Canadian cordillera on Vancouver Island [*Mayrand et al.*, 1987], and Death Valley, California [*Geist and Brocher*, 1987]. These studies allow better understanding of reflection events observed from the middle and lower continental crust [*Brocher*, 1981*b*; *deVoogd et al.*, 1986].

In February 1986 the U.S. Geological Survey (USGS) acquired 107 km of deep crustal seismic reflection data along a N-S trending profile which followed the Richardson Highway in south central Alaska. These data were collected in support of the Trans-Alaska Crustal Transect (TACT), a comprehensive geological and geophysical study of the crust within a corridor across Alaska [*Page et al.*, 1986]. In this paper we discuss the Chugach reflection line, which traversed northward across geological strike from the center of the Chugach Mountains into the Copper River Basin across a major fault bounding tectonostratigraphic terranes (Figure 1). This terrane boundary, the Border Ranges fault, is the main structural boundary between the Chugach terrane, south of the fault, and the Peninsular terrane, north of the fault [*Jones et al.*, 1984].

Recent hypotheses concerning the evolution of the continental crust of the Alaskan Cordillera and elsewhere emphasize the role of accretion of tectonostratigraphic terranes [*Coney et al.*, 1980; *Howell et al.*, 1985]. The main objective of the 1986 seismic reflection survey was to delineate the crustal structure beneath major terrane boundaries. Inasmuch as stacked sections of the deep seismic reflection data to date provide little new information on the Border Ranges fault itself, we examined the first arrivals on common shot gathers to obtain a high-resolution velocity structure of the shallow crust across this fault system.

In this report we present a high-resolution velocity model along the Chugach seismic reflection line and interpret the model geologically. The interpretation is based on the correlation of refraction velocities with rock velocities measured in the laboratory and with rock exposures. We relate aspects of the wave propagation exhibited by shallow guided waves to the quality of the deep crustal seismic reflection data. The high-resolution model is compared to a similar model derived from regional refraction data along the same line. The interpretation is further constrained by comparing the normal incidence reflection and refraction images of the shallow crust. Finally, the irregular geometry of the reflection line and the long recording array used to acquire the reflection section also allow us to test the hypothesis that a measureable velocity anisotropy exists within the Chugach terrane.

Paper number 7B5090.
0148-0227/89/007B-5090$05.00

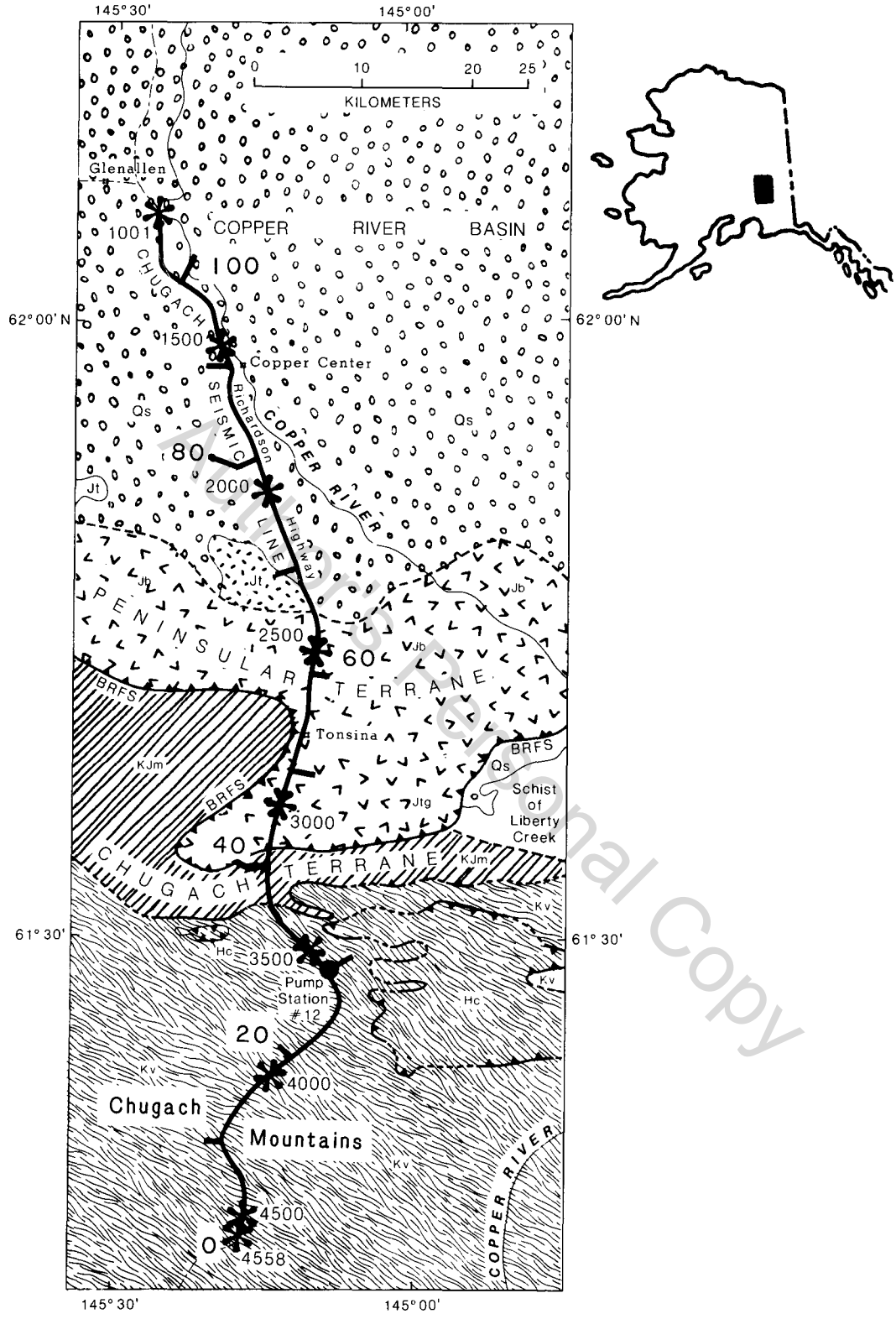

Fig. 1. Location map showing the study region as well as a more detailed map showing the geology in the area traversed by the Chugach seismic reflection line. Numbered (1001–4558) stars show vibrator points. Numbered (0–107) dashes show ranges in kilometers along the Chugach reflection line. Map features and map unit symbols used in this figure: BRFS, Border Ranges fault system; Hc, Haley Creek terrane, which includes Upper Paleozoic metamorphic rocks and Upper Paleozoic and Late Jurassic metaplutonic rocks; Jt, Lower Jurassic Talkeetna Formation, volcanic and volcaniclastic rocks; Jb, Nelchina River Gabbronorite; Middle Jurassic schist of Liberty Creek; Jtg, Tonsina ultramafic-mafic assemblage; KJm, Jurassic and Cretaceous McHugh Complex, a subduction melange; Kv, Upper Cretaceous Valdez Group, which includes mainly strongly deformed turbidite sequences and oceanic mafic volvanic rocks; Qs, Quaternary surficial deposits. The location of Pump Station 12 on the Trans-Alaska oil pipeline is shown as a large circle.

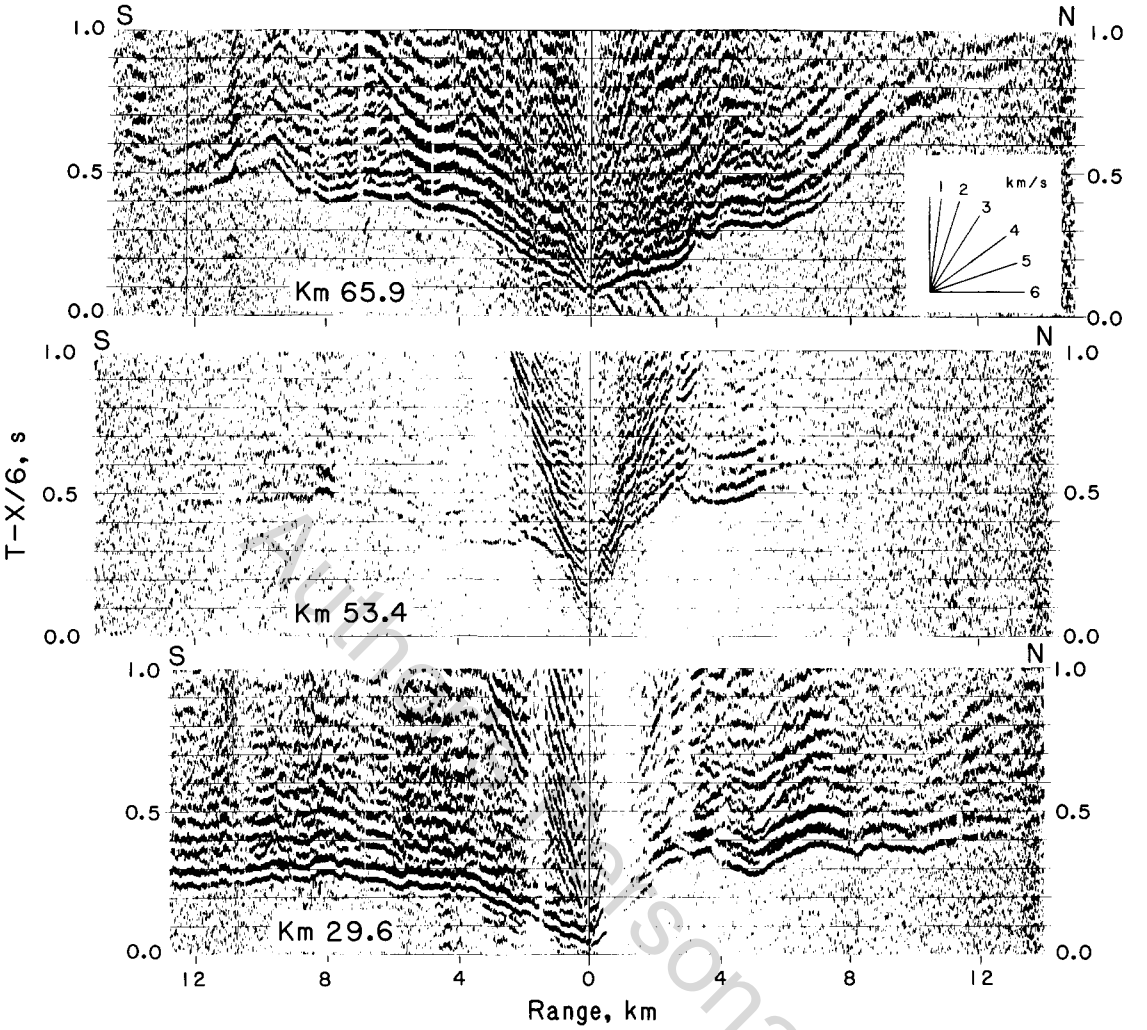

Fig. 2. Examples of common shot gathers used for the travel time analysis. Source-receiver ranges were calculated using the surveyor's locations for the geophone stations. As described in the text, the travel times have been linearly reduced using a velocity of 6 km/s, and the amplitudes have been corrected for geometrical spreading according to the square root of range. Numbers on the gathers indicate the locations of the vibrator point in kilometers along the Chugach reflection line (Figure 1). Large-amplitude guided waves can be observed as a tight cone nearest the source.

Collection and Processing of Seismic Reflection Data

Seismic reflection data along the Chugach line were collected for the USGS by Geophysical Systems Corporation, using a sign bit recording system and an array of Vibroseis (trade and service mark of Continental Oil Company) sources. Field acquisition parameters are described by *Fisher et al.* [this issue] and include a sweep between 10 and 30 Hz and a symmetrical split spread of 1024 geophone arrays spaced at 30-m intervals. Nominal shot-to-group offsets ranged from −15.36 to +15.36 km. These maximum offsets were not always achieved, however, owing to curvature of the road. No gap intervened between the source and first active groups of the spread, so that refracted arrivals from near-surface horizons are generally well recorded. The geophones were grouped into compact point rather than linear distributed arrays; low-velocity arrivals therefore were not degraded by the recording array. Sources were spaced at 120-m intervals along the line.

We plotted common shot gathers after correction for shot-geophone range, using the surveyed geophone and source locations. These ranges are accurate to within a meter. The amplitude of each trace was corrected for geometrical spreading by multiplying by the square root of the range. No other processing was performed on the gathers. Typical common shot gathers from along the Chugach line are shown in Figure 2.

Over 6800 travel times of first arrivals were digitized from common shot gathers along the line (Figure 3). Gathers were digitized for source points separated by approximately 3 km, which provided six to eight reversed measurements of the travel time beneath every surface location. Because the data were acquired with a correlated Vibroseis source, we chose the arrival time to be the time of the first amplitude maximum. Timing errors inherent in the recording instrumentation are considered negligible at 1 ms. Travel times were digitized from paper sections plotted at a scale of 22.17 cm/s; at this scale, one half the predominate period of the refracted energy is 0.5 cm. Since digitizing errors are less than one half a cycle, errors in digitizing travel times are estimated to be less than 25 ms.

The nonlinear geometry of the reflection line results in three-dimensional ray paths. Our two-dimensional ray theory algorithm required the approximation of the crooked reflec-

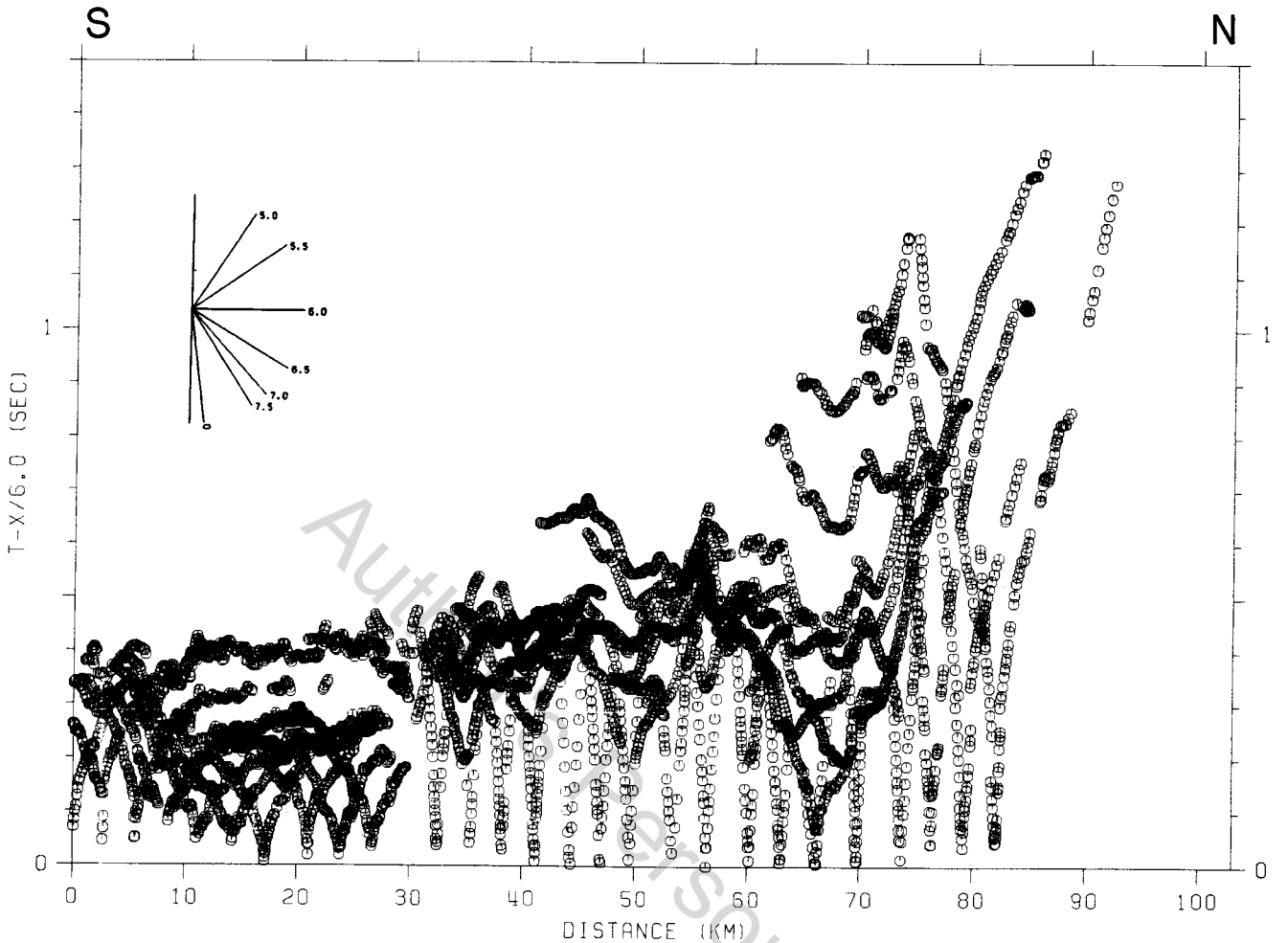

Fig. 3. Reduced (at 6.0 km/s) travel times used for vibrator points between km 0 and km 83. Additional travel time data (not shown) were used between km 83 and the northern end of the line. Note the dramatic increase in the observed travel times from south to north.

tion line to a linear transect. Instead of projecting the crooked reflection line onto the mean azimuth of the line, as is normally done in refraction studies, the two-dimensional approximation was achieved by straightening the reflection line by pulling the ends of the line taut. Specifically, this straightening was performed by calculating the location of each shot gather along the velocity depth model using the station number of the source and the nominal 30-m station spacing. In a similar manner, surveyed elevations accurate to within 1 m along the profile were incorporated into the velocity-depth model using the station number as an estimate of the range along the model. The advantage of this approach is that the resulting velocity model is easily correlated to the seismic reflection section itself. The accuracy of this approximation was checked by examining the surface consistency of the travel time curves plotted along the line as in Figure 3. As expected, the approximation was in greatest error where the reflection line is most crooked, near km 28 (Figure 1). Errors of a few hundred meters in these shot and elevation locations within the model near nonlinear portions of the reflection line probably explain some of the minor misfits of the calculated travel times with the observed travel times.

Although the high spatial density of observations makes this data set ideal for automatic one- and two-dimensional interpretive methods based on slant stacking [e.g., *Brocher*, 1981*a*; *Milkereit et al.*, 1985], the strongly two-dimensional structure limits the usefulness of these techniques. Time term (delay time) methods of analysis were also considered but were not applied owing to the significant variation in basement velocity along the line. In order to perform the least amount of processing of the data we chose to forward model the observed travel times with a two-dimensional velocity-depth structure using computer algorithms described by *Cerveny et al.* [1977] and *Hill et al.* [1985].

Initial velocity models were derived using two independent algorithms based on the observation that, very roughly, the arrivals could be characterized as originating from a 2.0 km/s layer over a 6.0 km/s half-space. In the first algorithm, intercept times of the arrivals having velocities close to 6 km/s were used to define the base of the 2 km/s surficial layer. In the second algorithm, two-way travel time picks of the base of the 2 km/s layer made from the stacked Chugach reflection section were converted to depth. Although the second algorithm provided an initial model yielding smaller travel time residuals than did the first algorithm, even that model required extensive revision before it provided an adequate match to the observed refracted first-arrival times.

During modeling, observed first-arrival travel times can be matched by varying either layer thickness or velocity or by varying both. For the uppermost layer of the model it was

necessary to vary the layer velocity as well as the layer thickness in order to match the observed first arrivals. For the deeper layers it was possible to obtain agreement between the observed and calculated travel times by varying primarily the layer thicknesses rather than the velocity within layers.

As discussed by many previous authors [e.g., *Hill et al.*, 1985], the uniqueness and resolution associated with the two-dimensional velocity-depth models which result from this forward, nonlinear modeling procedure are extraordinarily difficult to quantify. This is particularly true if the parameterization of the model has been too restrictive. Lacking orthogonally oriented profiles, for example, it is impossible to estimate the degree to which the two-dimensional models have been contaminated by out-of-the-plane propagation of seismic energy.

From trial and error perturbations in model parameters we believe that, on average, P wave velocities are resolved to within 5% and the depths to boundaries are resolved to within 10%. Given a sweep frequency content between 10 and 30 Hz, the shortest observable wavelengths in the near-surface layers having velocities of 2.0 km/s are 0.066 km and would increase to 0.2 km in rocks having P wave velocities of 6.0 km/s. If this is coupled with the average sensor spacing of 0.03 km, we may resolve, under optimal conditions, the position of lateral and vertical changes in near-surface structure to within several tens of meters. The position of lateral and vertical changes in structure at greater depths is probably resolved to within a few hundred meters. Figure 4, showing ray paths through the velocity-depth model, indicates that the resolution of the procedure differs along the model depending on the information density along the profile. Figure 4 illustrates that, on average, only the upper 1.5 km of the structure is sampled by ray paths, that the deeper structure immediately beneath a source point is not sampled by rays from that source, and that both ends of the profile lack reversed coverage, degrading the resolution of the procedure.

The uniqueness of the resulting velocity-depth model depends most importantly on the particular choices of phase correlation between arrivals and the choice of ray path and refracting horizon used to model these arrivals. To minimize the ambiguities associated with these choices, we analyzed common shot gathers separated by sufficiently small intervals, about 3 km, that the phase correlations could be interpolated from one source point to the next. Furthermore, the resulting velocity-depth model was required to compare favorably to the Chugach normal incidence reflection section itself. To compare the refraction model to the seismic reflection section, we calculated synthetic, normal incidence reflection times from the two-dimensional velocity-depth model.

SURFACE GEOLOGY

The following discussion of the near-surface geology along the Chugach seismic line is abstracted from descriptions of the outcrop geology near the study region presented by *Nichols and Yehle* [1969], *Winkler et al.* [1981], *Winkler and Plafker* [1981], *Jones et al.* [1984], *Plafker et al.* [1985, this issue], and *Nokleberg et al.* [this issue]. From south to north the Chugach line traverses the Chugach and the Peninsular terranes, which are in fault contact across the Border Ranges fault system (Figure 1).

The Chugach terrane near the transect consists of a northward succession of three sequences: the Valdez Group, the McHugh Complex, and the schist of Liberty Creek. All three sequences are bounded by faults and are strongly deformed by asymmetric, south verging folds and associated faults [*Winkler and Plafker*, 1981; *Plafker et al.*, this issue; *Nokleberg et al.*, this issue]. The schist of Liberty Creek may be faulted out near the surface just east of the transect (Figure 1). The sequences increase northward in age from Late Cretaceous to Middle or Early Jurassic. The Upper Cretaceous Valdez Group consists primarily of pelitic schist, metagraywacke, and metabasalt that have been metamorphosed to lower greenschist facies [*Winkler and Plafker*, 1981; *Winkler et al.*, 1981; *Plafker et al.*, this issue]. Metabasalt predominates in the structurally lowest (southernmost) part of the Valdez Group south of the area in Figure 1. The McHugh Complex is a subduction melange that includes mainly marine sedimentary and volcanic rocks. The melange matrix ranges in age from Late Triassic to mid-Cretaceous [*Winkler et al.*, 1981; *Plafker et al.*, this issue]. The schist of Liberty Creek consists of blueschist and greenschist facies rocks that are inferred to have Middle Jurassic metamorphic ages on the basis of comparisons of isotopically dated schist to the west [*Sisson and Onstott*, 1986; *Plafker et al.*, this issue].

The Border Ranges fault system bounds the northernmost outcrops of the Chugach terrane [*MacKevett and Plafker*, 1974; *Plafker et al.*, this issue]. In the vicinity of the Chugach line this fault system juxtaposes the McHugh Complex of the Chugach terrane against Jurassic ultramafic and mafic rocks that form the southernmost unit of the Peninsular terrane (Figure 1).

The Peninsular terrane consists mainly of the lower to middle Jurassic Border Ranges ultramafic-mafic assemblage [*Burns*, 1985; *Coleman and Burns*, 1985; *Plafker et al.*, this issue], as well as the Lower Jurassic Talkeetna Formation. Ultramafic and mafic rocks of the Tonsina ultramafic-mafic assemblage that form the lower part of the Border Ranges ultramafic-mafic assemblage are interpreted to have been emplaced at the base of an early to middle Jurassic oceanic island arc; they are overlain by a thick sequence of shallower level gabbros (Nelchina River Gabbronorite) north of the Border Ranges ultramafic-mafic assemblage [*DeBari and Coleman*, 1986, this issue]. The Lower Jurassic Talkeetna Formation and associated Middle and Late Jurassic intermediate plutonic rocks are regionally exposed [*Burns*, 1982, 1985]. The predominantly andesitic flows and volcaniclastic rocks in the lower part of this formation are overlain by sedimentary rocks and tuffs [*Winkler et al.*, 1981; *Burns et al.*, 1983]. The Talkeetna Formation is at least 2 km thick, is extensively faulted, and, in places, is broadly folded [*Winkler et al.*, 1981; *Plafker et al.*, this issue]. The Talkeetna Formation is in fault contact to the south with the Nelchina River Gabbronorite. The Copper River Basin, located on the northern end of the Chugach line (Figure 1), is filled by a thick sequence of Middle Jurassic to Upper Cretaceous clastic rocks deposited in a subaerial to deep marine environment; these Mesozoic rocks are in turn overlain by a thin veneer of Tertiary, predominately continental, sedimentary rocks [*Plafker et al.*, this issue].

A variety of unconsolidated Quaternary deposits are located along the Chugach reflection line. In the southern third of the line, glacial, alluvial, and minor fan deposits predominate, whereas in the northern two thirds of the line, glaciolacustrine sediments predominate with minor exposures of alluvium, slope deposits, and moraine sediments [*Nichols and Yehle*, 1969].

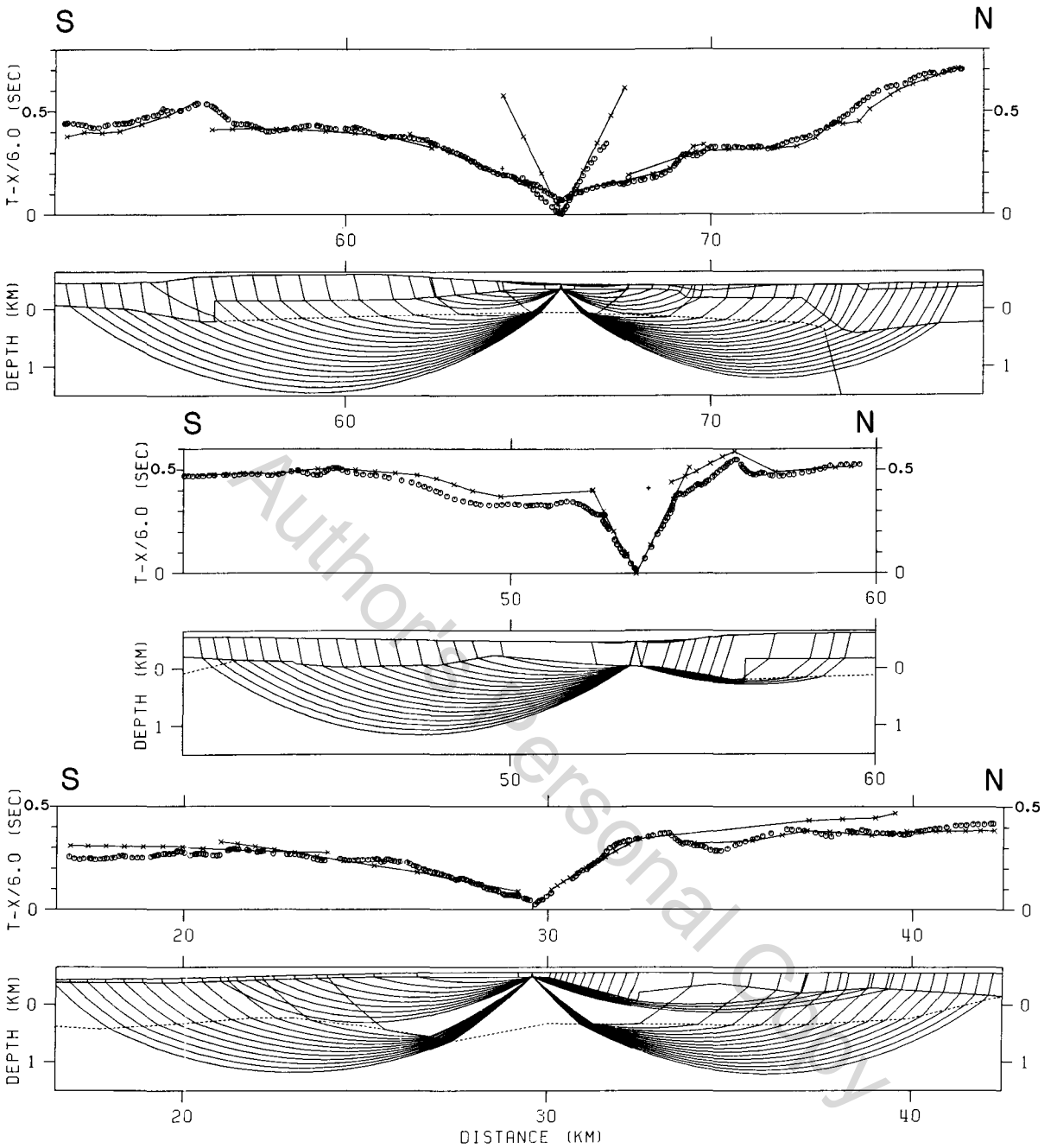

Fig. 4. Observed (circles) and calculated (crosses) travel times for the common shot gathers shown in Figure 2. Also shown beneath each travel time plot are ray paths through the appropriate velocity-depth structure. Such plots provide an indication of the subsurface coverage and show that only the upper 1.5 km of the structure is constrained by the first-arrival data.

The Refraction Model

Quaternary Deposits

The velocity-depth model inferred from the iterative forward modeling of reversed and overlapping travel times indicates that a layer, generally less than 500 m thick and having velocities between 1.1 and 2.1 km/s, is continuous along the entire Chugach reflection line (Figure 5). Because these velocities correlate to those expected for the Quaternary deposits described above (Table 1), we infer that this layer corresponds to Quaternary sediments.

The discontinuous, thin (100 m thick), and low-velocity (1.1–1.3 km/s) uppermost layer is an unusual but well-constrained feature of the model. Due to the deployment of the reflection geophone groups as point, rather than linear, arrays, the arrivals traveling at velocities as low as 1.1–1.3 km/s were not attenuated by the geophone groups. Arrivals from this layer are observed as direct waves, allowing the velocity of the layer to be determined without ambiguity. The lateral distribution of the layer is known chiefly by observation of the arrivals from the layer using source points distributed at 1- to 3-km intervals. Figure 5 indicates that this layer occurs where fan and coarse-grained alluvial deposits have been mapped.

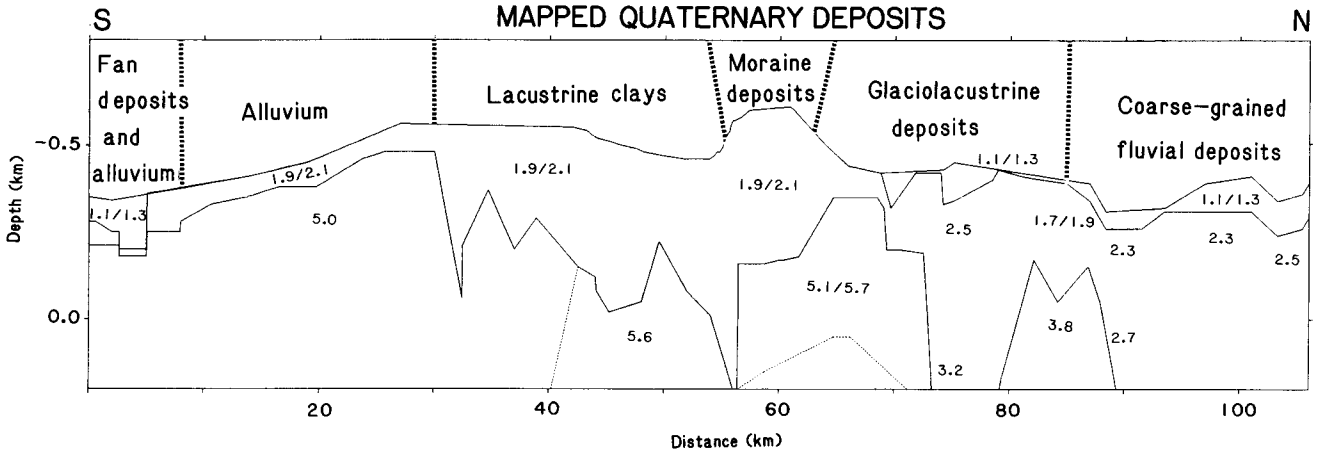

Fig. 5. Comparison of mapped Quaternary sediments by *Nichols and Yehle* [1969] and G. Plafker et al. (manuscript in preparation, 1988) with the uppermost portion of the velocity-depth model derived from the refracted first arrivals. Numbers on models indicate compressional wave velocities in kilometers per second.

A correlation between the mapped Quaternary deposits along the Chugach reflection line and the velocity and thickness of the uppermost layers in the refraction model is presented in Figure 5. The fan and alluvial sediments lying between Stuart (km 0) and Boulder (km 8) creeks thin northward, toward the Chugach Mountains. From km 8 to km 30 the thin layer of alluvium is confined to a narrow (200 m wide) belt of sediments in a U-shaped glacial valley [*Nichols and Yehle*, 1969; G. Plafker et al., unpublished data, 1987]. From km 30 to km 58, lacustrine clays lie along most of the reflection line in a more extensive 2-km-wide belt which is roughly defined by the 656-m contour on topographic maps and may explain the thickening of the 2.0 km/s layer in this region. Between km 58 and 61, moraine deposits outcrop and may underlie thin glaciolacustrine deposits between km 55 and 58 and between km 61 and 63. From km 63 to km 85, glaciolacustrine deposits within a broad basin underlie most of the reflection profile [*Nichols and Yehle*, 1969]. Coarse-grained fluvial deposits are exposed from km 85 to the northern end of the seismic line. These deposits probably account for an increased scatter of travel times noted in the Copper River Basin.

TABLE 1. Comparison of Laboratory and Refraction Measurements of Formation Compressional Wave Velocities

Unit	Previous Laboratory or Refraction Velocities,* km/s	Refraction Velocities From This Study, km/s
Surficial deposits		1.1–2.5
Till	0.8–1.8†, 0.3–2.4‡	
Frozen clay	2.02–4.11§	
Valdez Group		5.0–5.6
Phyllite	5.1	
Metagraywacke	5.7	
Metatuff	6.3	
Border Ranges		
Ultramafic-mafic assemblage	6.6	5.6
Talkeetna Formation		5.1–5.7
Andesite breccia	5.7	
Flow	6.1	

*Table 2.
†*Schon* [1983].
‡*Haeni* [1986].
§*Christensen* [1982, p. 141].

To investigate the influence of the surficial low-velocity layer on the quality of upper crustal reflections, we examined, as a function of shot location, the propagation of seismic wave energy guided within the 2.0 km/s layer. These arrivals, when present, normally consist of a series of multiple reflections and multiply reflected refractions whose velocities are asymptotic to that of the direct wave from the 2.0 km/s layer. The arrivals are not strongly dispersed and typically have frequencies of 12–17 Hz, corresponding to wavelengths of 120–170 m. We found significant variations in the efficiency of the generation and propagation of guided wave energy along the Chugach reflection line. Shot gathers selected at 1-km intervals show that these variations directly correlate with fluctuations in the thickness of the 2.0 km/s layer (Figure 6). Between km 0 and km 30 the guided waves are absent, whereas between km 30 and km 60 they have large amplitudes. For instance, at km 20.88, where the 2.0 km/s layer is about 100 m thick, there is essentially no guided wave energy. At km 43.92, where the 2.0 km/s layer is more than 400 m thick and is underlain by 5.6 km/s material, a strong set of guided wave arrivals is evident. The latter arrivals appear to be similar to the dispersed acoustic wave arrivals observed during the propagation of sound in shallow water. This observation suggests that techniques for investigating the acoustical properties of shallow water environments could be applied to the near-surface structure along the Chugach reflection profile [e.g., *Brocher and Ewing*, 1986]. In particular, the group and phase velocity dispersion curves of these arrivals could be inverted to place constraints on the velocity gradients within, and the thickness of, the 2.0 km/s layer.

The correlation between the thickness of the 2.0 km/s layer and the efficiency of guided wave energy propagation suggests at least two more mechanisms for explaining the poorer quality areas of the deep crustal reflection profile. The first and preferred explanation is that degradation of the reflection data by large-amplitude guided wave energy during stacking may have lowered the quality of the reflections in the upper 4 s of the crust. Processing of the reflection data to date has not included the filtering or muting of the high-amplitude guided waves and has relied upon the stacking process itself to reduce this energy. The second explanation is that regions of the line

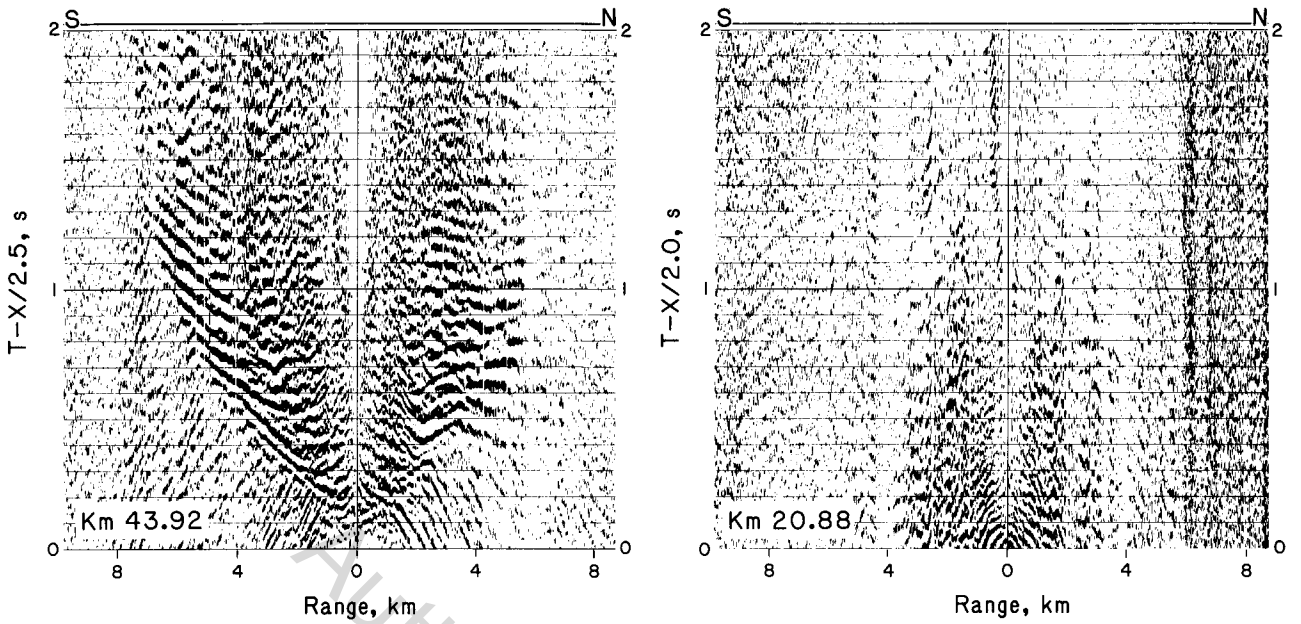

Fig. 6. Comparison of two common shot gathers plotted using linear reduction velocities of 2.0 and 2.5 km/s in order to better demonstrate the surface guided energy. Numbers on each gather provide its location in kilometers along the Chugach line. Note that the shot at km 20.88 is underlain by about 100 m of surficial sediment cover, whereas the shot at km 43.92 is underlain by more than 400 m of surficial sediments.

having thicker 2.0 km/s layers correspond to those having efficient guided wave energy. Thus more seismic energy is reflected at the base of this layer than where the layer is thinner, allowing less energy to be transmitted through the layer to deeper horizons.

The Deeper Structure

In this section we describe important features of the lower portion of the velocity-depth model inferred from the forward modeling. As previously described, the travel time data generally permit the resolution of refraction velocities to depths of about 1.5 km below the surface, although in the Copper River Basin, subsurface depths as large as 2.0 km were sampled.

The most pronounced feature of the velocity-depth model shown in Figure 7 is the steeply north dipping boundary at the southern end of the Copper River Basin, at km 73.5, well north of the Border Ranges fault system. Modeling of the dip of this boundary indicates that the best match to the observed travel times is obtained when the dip is close to 50°, although northward dips as low as 39° and as high as 68° produce less accurate but reasonable matches. In agreement with the regional refraction results reported by G. S. Fuis et al. (Crustal structure of the Chugach, Peninsular, and Wrangellia terranes, southern Alaska, submitted to *Journal of Geophysical Research*, 1988, hereinafter referred to as submitted manuscript, 1988) the boundary at the southern end of the Copper River Basin represents the largest change in near-surface velocity structure along the entire Chugach reflection line. South of the boundary, there is only a thin veneer of inferred sediments having velocities less than 5.0 km/s. North of the boundary the thickness of material having velocities less than 5.0 km/s increases to 2 km. Significant differences in wave propagation north and south of this boundary are illustrated in Figure 8, which shows a common shot gather from a source located directly over the boundary. Owing to the significant differences in the velocity model north and south of this boundary, we discuss these regions separately in the following discussion of the model.

Velocity Structure South of the Copper River Basin

South of the Border Ranges fault a layer having velocities of 5.0–5.6 km/s lies intermittently beneath the inferred Quaternary deposits (Figure 7). The 5.0–5.6 km/s layer is thickest in the Valdez Group where phase velocities of 5.0–5.2 km/s are observed in first-arrival times (Figures 2–3). This layer is also present near km 65.9, where phase velocities of 5.1–5.3 km/s are observed in the first arrivals for source-receiver ranges of 2-3 km (Figure 3). Although this intermediate-velocity layer was unresolved from the observed travel times for ranges between 42 and 59 km, where the Border Ranges ultramafic-mafic rocks are projected to occur, trial and error modeling indicated that the layer may be present but undetected if it is less than 100 m thick.

Low-amplitude but spatially coherent refracted shear wave arrivals are observed on several common shot gathers acquired within the Valdez Group. Shear wave velocities for five reversed gathers located between km 13.2 and 24.78 are approximately 3.3 km/s. This shear wave velocity would be appropriate, assuming a Poisson's ratio of 0.25, for the 5.0–5.6 km/s layer in the Valdez Group.

For the model south of the Copper River Basin the half-space underlying the 2.0 km/s and 5.0–5.6 km/s layers has a velocity gradient of approximately 0.3 km/s/km, which is sufficient to allow the rays to bottom and refract upward back to the surface. Although we used a few trial velocity gradients when modeling this half-space, no particular significance should be attached to the magnitude of the velocity gradient assigned to the half-space.

Velocity Structure Within the Copper River Basin

The velocity-depth model for the Copper River Basin indicates structural complexity within the basin (Figure 7). Be

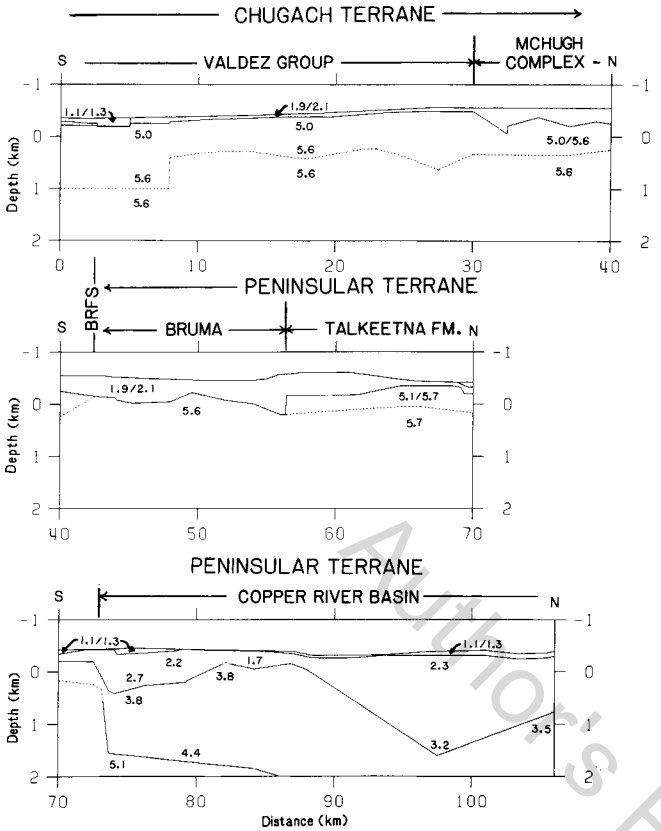

Fig. 7. The velocity-depth model derived from the fitting of first-arrival times with velocities in kilometers per second. The distribution of geologic formations as mapped at the surface is also indicated on the figure.

tween km 73.5 and 89 the observed travel times have been modeled using a layer of 1.7–2.7 km/s material ranging in thickness from 250 to 375 m. An abrupt offset in the base of this model layer correlates in location with an offset in the base of the 1.1–1.3 km/s layer, suggesting that the thicknesses of both the 1.2 and 1.7–2.7 km/s layers are fault controlled. Alternatively, the apparent offset in the base of the 1.7–2.7 km/s layer could be explained by further thickening the 1.2 km/s layer, suggesting that only the thickness of the uppermost layer is fault controlled.

The layer beneath this 1.7–2.7 km/s layer has velocities between 3.5 and 4.4 km/s and is nearly 2 km thick. The lower layer is best constrained in the model range interval km 73.6 to 88.6 within the Copper River Basin, where the overlying 1.7–2.7 km/s layer is relatively thin. The minimum thickness of the 3.5–4.4 km/s layer is constrained by the requirement that calculated wide-angle reflections from the base of the layer cannot precede the observed first arrivals. The maximum depth to the base of this layer, however, is poorly constrained by first-arrival data.

North of km 89, within the floodplain of the Copper River, the observed travel times reveal no evidence for seismic velocities in the second layer less than 2.3 km/s. Indeed, the observed travel times are best explained by a large linear velocity gradient within this layer between velocities of 2.3 and 3.2 km/s. Near km 97 the 2.3–3.2 km/s layer is about 1.8 km thick, and in this location the geometry of the layer resembles a V-shaped basin. At the northern end of the Chugach reflection line the lack of reversed refraction coverage does not allow the precise definition of the base of this layer with confidence. The lowermost layer has a seismic velocity of 3.5–4.4 km/s.

GEOLOGICAL INTERPRETATION

Compressional and shear wave velocities have been measured as functions of hydrostatic pressure for several Chugach-Peninsular basement rocks collected from exposures along the Richardson Highway using a pulse transmission technique described in detail by *Christensen* [1985]. Velocities were obtained for three mutually perpendicular directions from each rock type. Bulk densities and velocities averaged over the three directions are presented in Table 2 for several

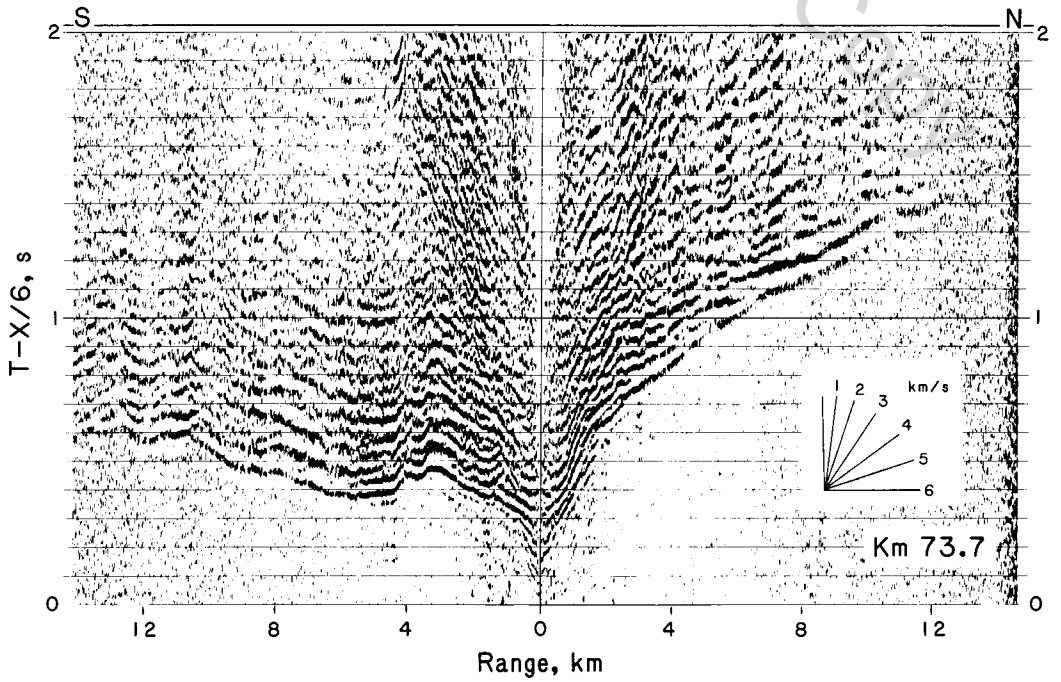

Fig. 8. Common shot gather with the vibrator point at km 73.7, directly over the major velocity boundary at km 73.5. As for Figure 2, the travel times for this gather have been linearly reduced using a velocity of 6.0 km/s. Note that asymmetry in propagation north and south of the source.

TABLE 2. Compressional (V_p) and Shear Wave Velocities (V_s) as a Function of Pressure (P)

Rock Type	Unit	Density, kg m^{-3}	Mode	P 10 MPa	50 MPa	100 MPa	200 MPa	400 MPa	600 MPa	800 MPa
Phyllite	Valdez Group	2723	V_p	5.14	5.57	5.82	6.08	6.28	6.36	6.14
			V_s	3.02	3.23	3.36	3.48	3.58	3.61	3.64
Metagraywacke	Valdez Group	2716	V_p	5.66	6.02	6.12	6.19	6.25	6.29	6.32
			V_s	3.58	3.69	3.73	3.76	3.78	3.79	3.80
Metatuff	Valdez Group	2779	V_p	6.25	6.51	6.58	6.64	6.70	6.73	6.76
			V_s	3.34	3.41	3.44	3.47	3.51	3.52	3.54
Serpentinized dunite	Tonsina Complex	2984	V_p	6.62	6.69	6.73	6.79	6.87	6.93	6.98
			V_s	3.56	3.61	3.62	3.64	3.67	3.69	3.70
Andesite breccia	Talkeetna Formation	2686	V_p	5.71	5.96	6.08	6.20	6.29	6.34	6.37
			V_s	3.42	3.54	3.60	3.64	3.67	3.69	3.70
Andesite flow	Talkeetna Formation	2886	V_p	6.12	6.37	6.48	6.56	6.64	6.68	6.71
			V_s	3.54	3.63	3.67	3.70	3.73	3.74	3.76

Velocities are in kilometers per second.

major lithologies underlying the seismic traverse. In the following discussion, the laboratory measurements are compared with our velocity models for the Chugach and Peninsular terranes.

South of the Border Ranges fault, basement rocks underlying the 2.0 km/s layer have velocities of 5.0–5.6 km/s (Figure 7). The major exposed lithologies are phyllite, metagraywacke, and minor (less than 10%) metatuff. Compressional wave velocities of phyllite from the Valdez Group measured in the laboratory at low pressure and room temperature average 5.1 km/s. Similarly, a sample of Valdez Group metagraywacke has a mean compressional wave velocity of 5.7 km/s (Table 2). The metatuff is significantly faster, with compressional wave velocities averaging 6.3 km/s. Laboratory measurements of the shear wave velocities of these rocks ranged from 3.0 to 3.6 km/s (Table 2). Thus the refraction velocities determined for this layer are consistent with the predominant lithologies within the Valdez Group.

Bedrock velocities ranging from 5.0 to 5.6 km/s under the projected location of the McHugh Complex along the model are not significantly different from those of the Valdez Group (Figure 7). The projected location of the McHugh Complex, however, proved to be one of the most difficult areas in which to obtain agreement with observed travel times using the velocity-depth model shown in Figure 7, owing to the sharp bend of the reflection line at km 28. The assumption of a constant distance of 30 m between stations is least appropriate for this portion of the model, and there is strong evidence for a significant velocity anisotropy within the basement rocks in this location (see below).

The projected location of the Border Ranges fault corresponds to the northern truncation of the 5.0–5.6 km/s layer at km 42. North of the Border Ranges fault the model shows that the 2.0 km/s layer rests directly on rocks having velocities greater than 5.6 km/s. A dunite containing approximately 25% serpentinite from near the base of the Tonsina ultramafic-mafic assemblage has a laboratory compressional wave velocity of 6.6 km/s at low pressure and room temperature (Table 2). With increasing serpentinization, velocities in ultramafic rocks decrease to approximately 5.0 km/s for completely serpentinized peridotite [*Christensen*, 1982, pp. 144–191]. Thus the observed velocities in the Tonsina ultramafic-mafic assemblage suggest appreciable serpentinization at depth. In addition, the velocities will be dependent upon the ratio of gabbro to ultramafic rocks in the complex.

Prominent vertical offsets of the base of the 2.0 km/s layer in the Tonsina ultramafic-mafic assemblage and the Nelchina River Gabbronorite may either represent reactivated splay faults of the Border Ranges fault system or unrelated later faulting. We believe these offsets document reactivation of faults rather than the original motion, since the Border Ranges fault system is thought to have been most active in the late Mesozoic. The offset at km 57 is particularly prominent, showing 350 m of apparent vertical displacement on the base of the 2.0 km/s layer. This offset produces a large one-way travel time anomaly of close to 0.1 s, which exceeds the 0.025-s uncertainty of the travel times by a factor of 4. Although no laboratory rock velocities are available from the Nelchina River Gabbronorite, the high velocities in the model are consistent with those of other gabbros [*Christensen*, 1982, pp. 144–191].

Where the Talkeetna Formation outcrops, the velocity model indicates a shallow layer having velocities between 5.1 and 5.7 km/s. Measured compressional wave velocities of an andesite breccia and a flow from the Talkeetna Formation at 10 MPa are 5.7 and 6.1 km/s, respectively (Table 2). Because the andesite breccia is the more common lithology within the Talkeetna Formation, the laboratory measurements are compatible with the refraction velocities.

The most prominent structural boundary along the entire Chugach profile is the northward dipping offset at km 73.5. From its location we infer that this boundary represents the southmost large-scale fault defining the Copper River Basin. On the basis of sonic and other geophysical logging results from within the Copper River Basin north of Glennallen (E. L. Ambos et al., Seismic refraction measurements within the Wrangellia-Peninsular (Composite) Terrane, south central Alaska, submitted to *Journal of Geophysical Research*, 1988, hereinafter referred to as submitted manuscript, 1988), the entire section within the Copper River Basin having velocities less than 4.4 km/s represents Upper Jurassic and Lower Cretaceous and younger sedimentary rocks. In the Ahtna wells, just north of Glenallen, about 300 m of Tertiary nonmarine Miocene(?) strata overlie 1600 m of Cretaceous marine strata (C. E. Kirschner, unpublished data, 1987). The Lower and Upper Cretaceous Matanuska Formation, consisting of moderately indurated marine siltstones and sandstones, has sonic well velocities between 2 and 3 km/s (E. L. Ambos et al., submitted manuscript, 1988). With higher degrees of induration, sonic velocities within the Matanuska Formation are

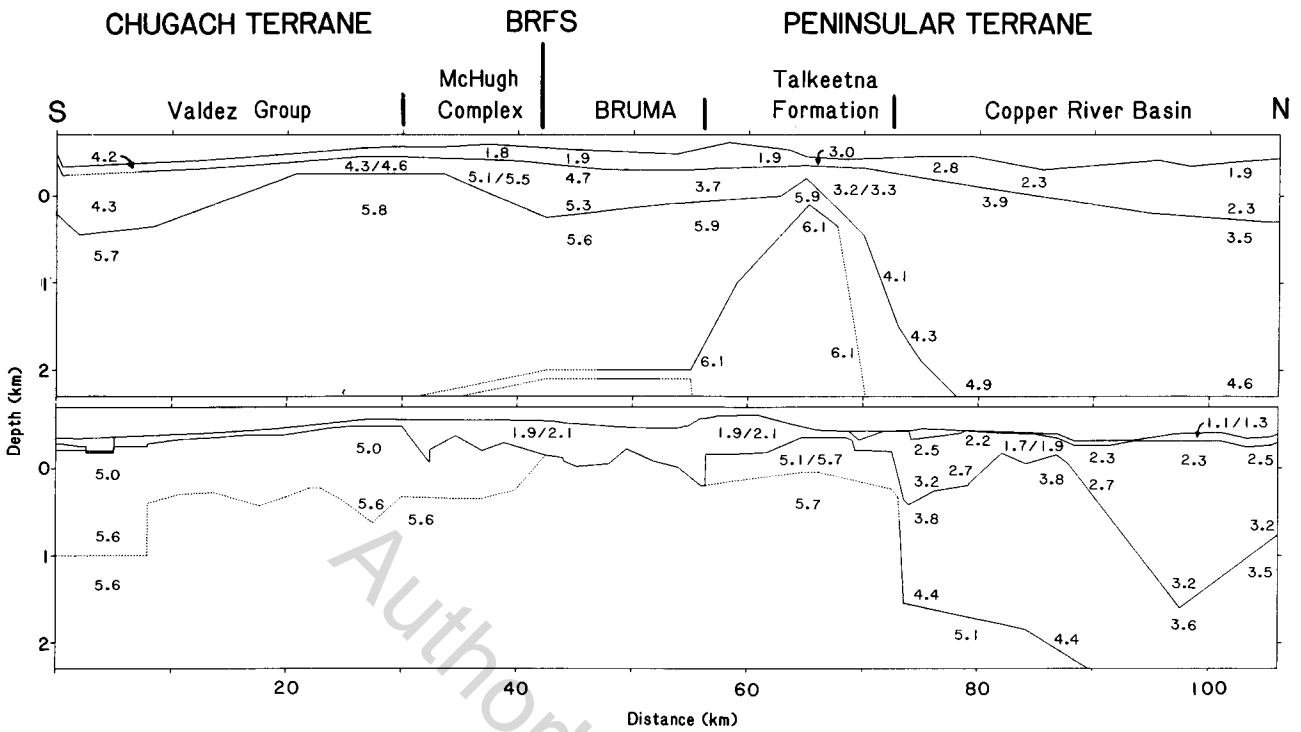

Fig. 9. Comparison of velocity-depth models for the Chugach reflection line based on (top) a regional refraction line (G. S. Fuis et al., submitted manuscript, 1988), and (bottom) the Chugach reflection line. Numbers on the model indicate velocities in kilometers per second. Symbols used in this figure: BRFS, Border Ranges fault system; BRUMA, Border Ranges ultramafic-mafic assemblage.

slightly in excess of 3 km/s. The Matanuska Formation is underlain by more indurated rocks having essentially the same lithology, which may explain the observed refraction velocity increase from 3.2 to 3.5 km/s within the basin. The interpretation of this entire section as moderately well lithified sedimentary rocks is consistent with the relatively poor propagation of compressional wave energy within the Copper River Basin.

Directly north of the offset at km 73.5, the 1.7–2.7 km/s layer may represent Paleocene and Eocene sediments shed northward during the uplift of the Chugach Mountains. These Paleocene and Eocene sediments, known as the Chickaloon Formation (an unconsolidated nonmarine conglomerate having shale and minor coal units), would have velocities appropriate for this layer of the model.

Comparison to a Regional Refraction Model

A primary objective of the TACT study is the determination of the crustal structure beneath the accreted terranes to Moho depths. Critical to this objective is the acquisition of regional refraction lines up to 240 km long. These lines, acquired using explosive sources at 20- to 30-km intervals and recorded by receivers spaced at 1-km intervals, provide only a sparse sampling of the near-surface horizons. A comparison of the velocity models derived from the regional refraction line and the first-arrival analysis of the reflection data is presented in Figure 9. This comparison is achieved by projecting the model of G. S. Fuis et al. (submitted manuscript, 1988) onto the crooked road followed by the Chugach reflection line.

The two different velocity models presented in Figure 9 exhibit many similarities. The regional refraction and reflection velocity models locate the southern boundary marking the thickest accumulation of sediments within the Copper River Basin at km 70 and 73.5, respectively. The inferred Quaternary cover, while poorly constrained by the regional refraction survey, is thin for both models within the Chugach terrane, especially between km 8 and 30. The velocities of the basement rocks in the Valdez Group and the McHugh Complex range between 5.6 and 5.9 km/s for both models. Both models show a thin sediment cover over the Talkeetna Formation from km 65 to 69. In both models the velocities in the basement of the Talkeetna Formation are higher than those of the Valdez Group.

Both velocity models indicate that the Copper River Basin is floored by a thick section of rocks having velocities less than 5 km/s. These models are consistent with previous interpretations of gravity and magnetic anomaly data from the Copper River Basin [*Andreasen et al.*, 1964]. The near-surface velocities in the Copper River Basin vary laterally in both models. There is, however, no structure in the regional refraction model resembling the not fully constrained V-shaped basin at km 97 in the reflection model.

We conclude that while the velocity model based on high-resolution refraction data shows greater structural detail than does the model based on the regional refraction lines, the models show broad similarities. This agreement demonstrates that the regional refraction profiling provides useful constraints on the structure within the first few kilometers in depth and lends further support for the models for the lower crust derived from these regional refraction data. We plan to incorporate the more detailed model presented here into the regional refraction models to gain greater confidence in the lower crustal models.

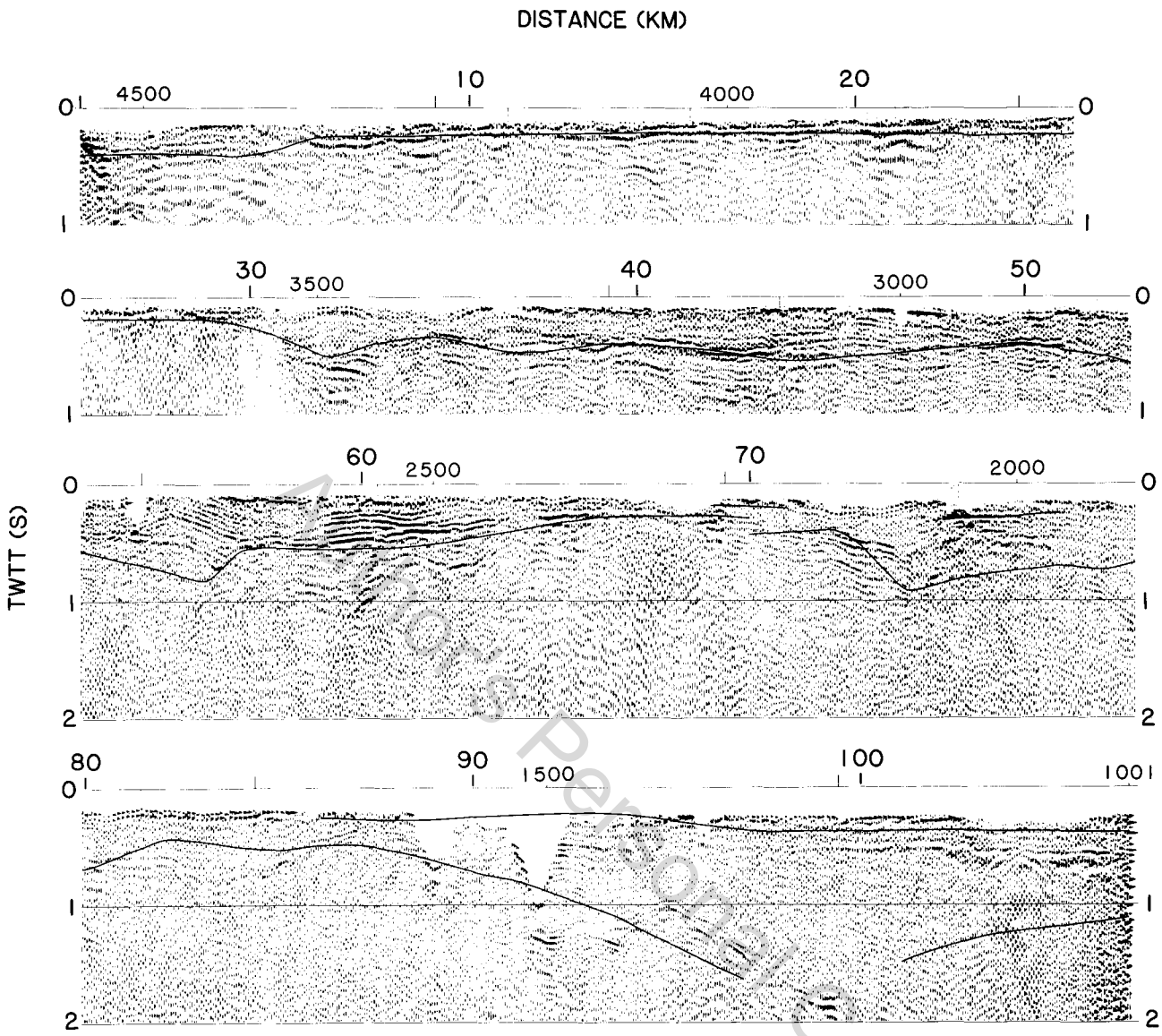

Fig. 10. Comparison of synthetic travel times (shown as solid lines) calculated from the velocity-depth model shown in Figure 7 with the uppermost portion of the Chugach seismic reflection section. Numbers along the section are the vibrator point locations provided in Figure 1.

Comparison of the Velocity Model to Vertical Incidence Reflection Profiles

The Chugach reflection section exhibits reflections from the shallow crust (upper hundred meters). Because the base of the 1.2, 2.0, and 3.2 km/s layers in the velocity model may be strong reflectors, we have compared the Chugach reflection profile to a synthetic reflection section calculated from our velocity model. Comparison of the times predicted from a synthetic reflection section with the unmigrated Chugach seismic reflection section (Figure 10) shows that the reflection times predicted from the model in Figure 7, assuming vertical incidence (not vertical propagation), generally agree with the observed reflection time to within 100 ms two-way travel time (twtt), which corresponds to a discrepancy in depth of less than 50 m for the 2.0 km/s layer. Since we did not attempt to model topography less than 50 m at the base of the 2.0 km/s layer, the agreement between the predicted and observed reflection times is within reasonable accuracy. The observed shoaling of reflections between km 8 and 29 (VP 3550 to 4300) is well matched by the synthetic travel times, as they are also between km 67 and 69 (VP 2150 and VP 2255). The vertical offset of reflection times observed in the Chugach reflection section at km 57 (VP 2650) is seen in the refraction model, but the details of the observed profile are not resolved by the subset of the refraction data analyzed. Reflections from the base of the 1.2 km/s layer in the Copper River Basin (VP 1001 to VP 1650) are also fit by the refraction-based model. The transition within the Copper River Basin between the base of the 2.3–3.2 km/s layer and the top of the 3.5–4.4 km/s layer is also reflective (VP 1300 to VP 1650) and matches the predicted reflection times. Generally, however, few reflections stem from within the basin, suggesting that the sedimentary fill is either poorly bedded, poorly sorted, highly indurated, or highly deformed.

Another motivation for this study was to search for geological explanations for the lateral variations in the quality of

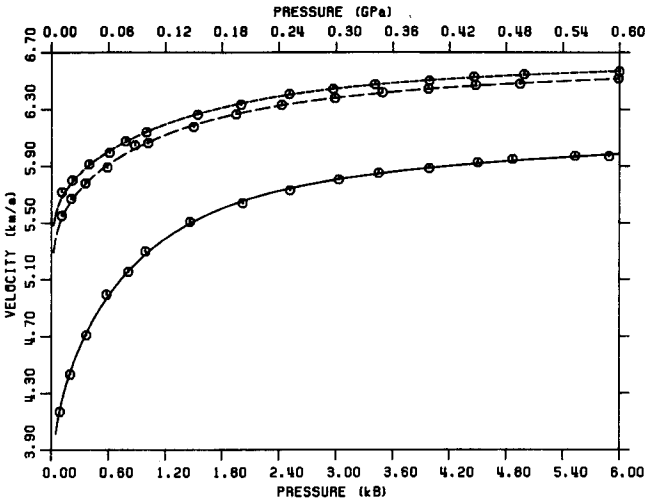

Fig. 11. Laboratory measurements of velocities (circles with tick-marks) in a phyllite from the Valdez Group measured normal (solid curve) and parallel (dashed curves) to foliation.

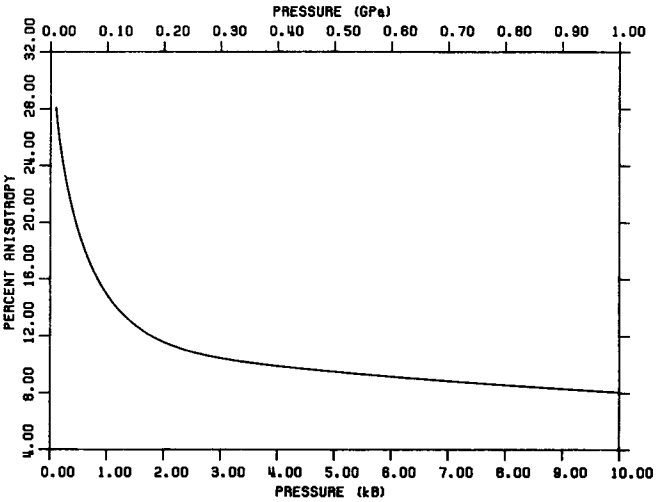

Fig. 12. Percent anisotropy of a phyllite from the Valdez Group as a function of pressure.

midcrustal to lower crustal reflections in the Chugach section. The largest-amplitude near-vertical reflections from midcrustal depths of 5–9 s twtt on the Chugach seismic reflection section are located between km 8 and 38 [*Fisher et al.*, this issue], where the thickness of the overlying 2.0 km/s layer is generally less than 200 m (Figure 5). To the north and south of this range interval the amplitudes of deep near-vertical reflections decay monotonically over a distance of about 8 km until they can no longer be observed. The thickening of the 1.1–1.3 km/s layer south of km 8 (Figure 5) correlates with reduced amplitudes of midcrustal reflections. However, in this area, we believe that the amplitude reduction is most plausibly explained by the gradual loss of fold of the stacked section southward of km 8. Because the reflection spread was 15 km long on a side, we believe that the thickening of the 2.0 km/s layer north of km 30 best explains the apparent loss of deep crustal reflection events on the Chugach section north of km 38. Correlations of midcrustal to lower crustal reflector quality with variations in near-surface sediments in other localities [*Stewart et al.*, 1986; E. R. Flueh, personal communication, 1987] suggest that the thickness of the 1.9–2.1 km/s layer controls the data quality of the near-vertical reflection section.

Velocity Anisotropy

High-resolution refraction analysis of the LITHOPROBE reflection lines on Vancouver Island indicate a pronounced velocity anisotropy in the Leech River Complex [*Mayrand et al.*, 1987], a Mesozoic accretionary melange [*Fairchild and Cowan*, 1982]. Laboratory measurements at room pressure and temperature of phyllitic rocks suggest that significant velocity anisotropy is present within the Valdez Group in the Chugach Mountains. Compressional wave velocities are shown as a function of pressure in Figure 11 for three mutually perpendicular propagation directions in a sample of Chugach phyllite. The lower velocities were measured normal to foliation, whereas the two dashed curves show velocities measured within the foliation plane. In Figure 12 the percent anisotropy has been calculated from the velocity curves of Figure 11. At pressures above 0.20 GPa the anisotropy primarily originates from preferred mineral orientation within the phyllite. At lower pressures, microcracks oriented subparallel to the foliation also contribute to the anisotropy [*Christensen*, 1965]. Thus the initial rapid decrease in phyllite anisotropy with increasing pressure shown in Figure 12 originates from decreasing crack porosity. The Valdez Group between km 18 and 35 includes strongly folded rocks, whose fold axes strike E-W. Inasmuch as the slowest direction in the laboratory measurements is perpendicular to the bedding plane, the fastest velocities should be oriented E-W, and the slowest direction should be N-S.

A fortuitous combination of the crooked geometry of the reflection line and the 15-km length of the reflection spread allowed us to determine whether a measureable velocity anisotropy exists within the near-surface Valdez Group rocks. As can be seen in Figure 1, the reflection line bends sharply within the Valdez Group at km 28, where segments of the line have an orientation of $\pm 45°$ from north. Thus some sources on one side of the bend have some receivers on the other side. We therefore compared the velocities obtained along the road segments having a NE-SW orientation to those determined for purely N-S oriented paths. N-S paths were obtained by selection of appropriate source and receiver pairs for sources between km 19 and 35. Reduced travel times for these picks are plotted in Figure 13. The travel times have been corrected for variations in the thickness of the 2.0 km/s layer, using thicknesses determined from Figure 7. There also exists about 100 m topographic relief along this portion of the profile. An additional approximate correction for the 100-m difference in elevation of the data from km 19 to km 24 was estimated assuming vertical propagation of the seismic energy at 5.0 km/s. The velocity obtained from these picks is 5.18 ± 0.09 km/s without the correction for elevation variations and is 5.11 ± 0.10 km/s with this correction. Thus elevation corrections lower the apparent velocity of energy propagating N-S.

The range of in situ refraction velocity estimates for N-S azimuths is consistent with a significant velocity anisotropy within the Chugach terrane. The N-S velocity, determined with corrections only for variations in the thickness of the uppermost sediments, is significantly lower than that determined for the NE-SW azimuth at ranges greater than 5 km. The NE-SW velocity at ranges greater than 5 km is essentially 6.0 km/s (Figure 13), corresponding to an anisotropy of 14%, which is reasonable considering an anisotropy less than 20%

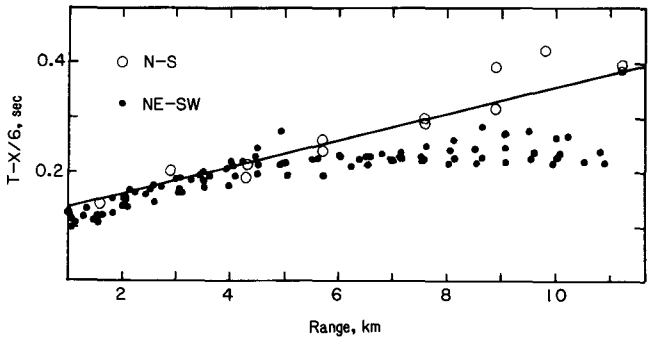

Fig. 13. Reduced travel times for N-S and NE-SW oriented paths around the bend in the reflection line in the Chugach Mountains, plotted as a function of source-receiver offset. As described in the text, the N-S travel times have been corrected for variations in the thickness of the 2.0 km/s layer. A linear regression of these travel times indicates that the apparent velocity along these paths is 5.18 ± 0.09 km/s, significantly lower than the 6.0 km/s observed on NE-SW azimuths, indicating an anisotropy of 14%.

would be expected for this orientation. The data in Figure 13 and our velocity model suggest that this anisotropy begins at a depth of 1 km within the Valdez Group, where the rocks are more competent and less fractured. Unlike the laboratory measurements of hand samples, the in situ measurements reported here show no anisotropy of the near-surface rocks, suggesting that these rocks contain large-scale fractures that obscure the anisotropy. As regional-scale refraction profiling within the Chugach terrane has also determined a velocity anisotropy with the identical orientation (G. S. Fuis et al., submitted manuscript, 1988), seismic experiments specifically designed to examine the anisotropy within the Valdez Group may be useful in refining these azimuthal and depth variations.

Discussion

The most significant structural boundary interpreted from the velocity-depth model is the north dipping interface delineating the southern limit of the Copper River Basin at km 73.5 (Figure 7). The absence of mapped normal faults in this portion of the basin [*Nichols and Yehle*, 1969] suggests that vertical deformation along this interface is not active. For this reason, the interface at km 73.5, whose geometry suggests a throw of at least 1300 m, is inferred to be a relict (buried) normal fault juxtaposing sedimentary rocks in the Copper River Basin and the Talkeetna Formation. A 0.3-km vertical offset in the opposite sense located 15 km south at km 57 would appear to make a horst block out of the Talkeetna Formation (Figure 7).

The Border Ranges fault is expressed in at least two ways. First, the Border Ranges fault zone is expressed at km 57 by a vertical offset. Second, the location of the Border Ranges fault is marked at km 42 by the juxtaposition of slower basement rocks within the McHugh Complex to the south against faster basement rocks of the Tonsina ultramafic-mafic assemblage to the north. The subsurface location of the Border Ranges fault closely matches the projection of the fault at km 42 shown in Figure 1 but not the offset at km 57. The offset at km 57 may thus reflect reactivation of a Border Ranges fault or an unrelated stage of later deformation. The offset at km 57 lies about 2 km to the north of the projected location of the contact between the Tonsina ultramafic-mafic assemblage and the Nelchina River Gabbronorite, which is based on isolated outcrops located 4 to 5 km from the Chugach reflection profile [*Plafker et al.*, this issue]. The up-to-the-north sense of motion on offset agrees with that of the Border Ranges fault in this area and elsewhere [*Nokleberg et al.*, this issue].

The Border Ranges fault zone requires no significant velocity anomaly to fit the observed travel times. This finding could mean either that the fault zone is thin or that the zone lacks a sizeable velocity contrast with the surrounding country rock. A wide (1–2 km) low-velocity fault zone, however, is inconsistent with the travel time modeling.

Summary

A high-resolution refraction study of several thousand first arrivals on large-aperture reflection field records was undertaken to help place constraints on the structural relations of accreted terranes in southern Alaska. Travel times of the first arrivals were modeled using iterative two-dimensional ray tracing and resulted in a velocity depth model along the Chugach reflection line. Evidence of anisotropy in seismic velocity of 0.8 ± 0.1 km/s in the Valdez Group was determined (14%) with the slow direction oriented N-S and the fast direction oriented NE-SW, in agreement with laboratory measurements of seismic velocities and field relations within the Valdez Group. The actual anisotropy within the Valdez Group is likely to be higher in the E-W direction.

An inverse relation was noted between the quality of the deep seismic reflections and the thickness of the uppermost layer composed of alluvium and other unconsolidated Quaternary sediments. A thicker (more than 200 m thick) surficial layer was accompanied by larger-amplitude guided waves and lower-amplitude midcrustal reflections. While we are currently attempting to understand better the origin of this correlation, a possible explanation is that the combined effects of higher intrinsic attenuation, increased guided wave energy noise within the thicker surficial sediments, and random time shifts (statics) degraded the deep crustal reflection data relative to regions with less extensive sediment cover.

Finally, locations of contrasting basement velocities within the model correlate to projected contacts between distinct lithologies and/or formations. One such contact may mark the subsurface location of the Border Ranges fault, which has no expression in the Chugach reflection section. To the north, a reactivated splay of the Border Ranges fault system may be represented by a prominent 350-m vertical offset of the basement surface. The southern boundary between the sedimentary strata filling the Copper River Basin is defined by a north dipping interface between these low-velocity sedimentary units and the higher-velocity Lower Jurassic Talkeetna Formation. We infer at least 1300 m of dip-slip motion along this interface.

We plan to extend this modeling to include reflections from the midcrust in order to learn whether accurate constraints on the geometry and velocity of the upper crust can be obtained in this manner. We also plan to reprocess the Chugach reflection profile in order to test the hypothesis that the unmuted guided wave energy significantly degraded the reflected energy from upper crustal depths.

The field parameters used for the acquisition of the Chugach reflection line allow us to develop a well-constrained velocity-depth model for the upper 1–2 km of the crust using first-arrival travel times. The close receiver spacing, large number of receivers, grouping of the receiver group arrays into point receivers, and sampling of the wave field near the source array permit us to resolve the structure of the Quater-

nary sediment cover in detail. This detail allows the pre-Quaternary crustal structure to be resolved with greater confidence than if the near-source portion of the wave field is not recorded. The field parameters employed thus provide an unusual capability to image crustal structure and should be considered for other study areas.

Acknowledgments. We thank J. Luetgert for writing and maintaining the two-dimensional ray theory software, W. Nokleberg and G. Plafker for sharing their geological insights, E. Ambos for many helpful discussions, and R. Catchings, J. Collins, G. Fuis, R. Page, and G. Plafker for reading early drafts of the manuscript. Critical comments by L. Mayrand, J. Orcutt, and an anonymous reviewer greatly improved sections of the manuscript. We acknowledge funding from the Deep Crustal Studies program of the USGS. The laboratory velocity measurements were supported by ONR contract N-00014-84-K-0207.

REFERENCES

Andreasen, G. E., A. Grantz, I. Zietz, and D. F. Barnes, Geologic interpretation of magnetic and gravity data in the Copper River Basin, Alaska, *U.S. Geol. Surv. Prof. Pap., 316-H*, 135–153, 1964.

Brocher, T. M., Shallow velocity structure of the Rio Grande rift north of Socorro, New Mexico: A reinterpretation, *J. Geophys. Res., 86*, 4960–4970, 1981*a*.

Brocher, T. M., Geometry and physical properties of the Socorro, New Mexico, magma bodies, *J. Geophys. Res., 86*, 9420–9432, 1981*b*.

Brocher, T. M., and J. I. Ewing, A comparison of high resolution seismic methods for determining seabed velocities in shallow water, *J. Acoust. Soc. Am., 79*, 286–298, 1986.

Burns, L. E., Gravity and aeromagnetic modeling of a large gabbroic body near the Border Ranges fault, southern Alaska, *U.S. Geol. Surv. Open File Rep., 82-460*, 1982.

Burns, L. E., The Border Ranges ultramafic and mafic complex, south-central Alaska: Cumulate fractionates of island-arc volcanics, *Can. J. Earth Sci., 22*, 1020–1038, 1985.

Burns, L. E., T. A. Little, R. J. Newberry, J. E. Decker, and G. H. Pessel, Preliminary geologic map of parts of the Anchorage C-2, C-3, D-2, and D-3 quadrangles, Alaska, scale 1:250,000, *Alaska Div. Geol. Geophys. Surv. Rep. Invest., 83-10*, 3 sheets, 1983.

Cerveny, V., I. A. Molotkov, and I. Psencik, *Ray Method in Seismology*, 214 pp., Univerzita Karlova, Prague, Czechoslovakia, 1977.

Christensen, N. I., Compressional wave velocities in metamorphic rocks at pressures to 10 kbar, *J. Geophys. Res., 70*, 6147–6164, 1965.

Christensen, N. I., Seismic velocities, in *Handbook of Physical Properties of Rocks*, vol. II, edited by R. S. Carmichael, pp. 1–228, CRC Press, Boca Raton, Fla., 1982.

Christensen, N. I., Measurements of dynamic properties of rock at elevated pressures and temperatures, in *Measurements of Rock Properties at Elevated Pressures and Temperatures*, edited by H. J. Pincus and E. R. Hoskins, pp. 93–107, American Society for Testing and Materials, Philadelphia, Pa., 1985.

Coleman, R. G., and L. E. Burns, The Tonsina high-pressure mafic-ultramafic cumulate sequence, Chugach Mountains, Alaska, *Geol. Soc. Am. Abstr. Programs, 17*(6), 348, 1985.

Coney, P. J., D. L. Jones, and J. W. H. Monger, Cordilleran suspect terranes, *Nature, 288*, 329–333, 1980.

DeBari, S., and R. G. Coleman, Petrologic aspects of gabbros from the Tonsina complex, Chugach Mountains, Alaska: Evidence for deep magma chambers under an island arc, *Geol. Soc. Am. Abstr. Programs, 18*, 99, 1986.

DeBari, S., and R. G. Coleman, Examination of the deep levels of an island arc: Evidence from the Tonsina mafic-ultramafic assemblage, Tonsina, Alaska, *J. Geophys. Res.*, this issue.

deVoogd, B., L. D. Brown, and C. Merey, Nature of the eastern boundary of the Rio Grande rift from COCORP surveys in the Albuquerque Basin, New Mexico, *J. Geophys. Res., 91*, 6305–6320, 1986.

Fairchild, L. H., and D. S. Cowan, Structure, petrology, and tectonic history of the Leech River Complex, northwest of Victoria, Vancouver Island, *Can. J. Earth Sci., 19*, 1817–1835, 1982.

Fisher, M. A., T. M. Brocher, W. J. Nokleberg, G. Plafker, and G. Smith, Seismic reflection images of the crust of the northern part of the Chugach terrane, Alaska: Results of a survey for the Trans-Alaska Crustal Transect, *J. Geophys. Res.*, this issue.

Geist, E. L., and T. M. Brocher, Geometry and subsurface lithology of Southern Death Valley basin, California based on refraction analysis of multichannel seismic data, *Geology*, 15, 1159–1162, 1987.

Haeni, F. P., Application of seismic refraction methods in groundwater modeling studies in New England, *Geophysics, 51*, 236–249, 1986.

Hill, D. P., E. Kissling, J. H. Luetgert, and U. Kradolfer, Constraints on the upper crustal structure of the Long Valley–Mono Craters volcanic complex, eastern California, from seismic refraction measurements, *J. Geophys. Res., 90*, 11135–11150, 1985.

Howell, D. W., D. L. Jones, and E. R. Schermer, Tectonostratigraphic terranes of the circum-Pacific region, in *Tectonostratigraphic Terranes of the Circum-Pacific Region, Earth Sci. Ser.*, vol. 1, edited by D. W. Howell, pp. 3–30, Circum-Pacific Council for Energy and Mineral Resources, Houston, Tex., 1985.

Jones, D. L., N. J. Silberling, P. J. Coney, and G. Plafker, Lithotectonic terrane map of Alaska (west of the 141st meridian) part A, Lithotectonic Terrane Map of the North American Cordillera, edited by N. J. Silberling and D. L. Jones, *U.S. Geol. Surv. Open File Rep., 84-523*, A1–A2, 1984.

Jurdy, D. M., and T. M. Brocher, Shallow velocity model of the Rio Grande rift near Socorro, New Mexico, *Geology, 8*, 185–189, 1980.

MacKevett, E. M., and G. Plafker, The Border Ranges fault in south central Alaska, *J. Res. U.S. Geol. Surv., 2*, 323–329, 1974.

Mayrand, L. J., A. G. Green, and B. Milkereit, A quantitative approach to bedrock velocity resolution and precision: The LITHOPROBE Vancouver Island experiment, *J. Geophys. Res., 92*, 4837–4845, 1987.

Milkereit, B., W. D. Mooney, and W. M. Kohler, Inversion of seismic refraction data in planar dipping structure, *Geophys. J. R. Astron. Soc., 82*, 81–103, 1985.

Nichols, D. R., and L. A. Yehle, Engineering geologic map of the southeastern Copper River Basin, Alaska, scale 1:125,000, *U.S. Geol. Surv. Map, I-524*, 1969.

Nokleberg, W. J., G. Plafker, J. S. Lull, W. K. Wallace, and G. R. Winkler, Structural analysis of the southern Peninsula, southern Wrangellia, and northern Chugach terranes along the Trans-Alaska Crustal Transect, northern Chugach Mountains, Alaska, *J. Geophys. Res.*, this issue.

Page, R. A., G. Plafker, G. S. Fuis, W. J. Nokleberg, E. L. Ambos, W. D. Mooney, and D. L. Campbell, Accretion and subduction tectonics in the Chugach Mountains and Copper River Basin, Alaska: Initial results of the Trans-Alaska Crustal Transect, *Geology, 14*, 501–505, 1986.

Plafker, G., W. J. Nokleberg, and J. S. Lull, Summary of 1984 TACT geological studies in the northern Chugach Mountains and southern Copper River Basin, *U.S. Geol. Surv. Circ., 967*, 76–79, 1985.

Plafker, G., W. J. Nokleberg, and J. S. Lull, Bedrock geology and tectonic evolution of the Wrangellia, Peninsular, and Chugach terranes along the Trans-Alaskan Crustal Transect Alaska, *J. Geophys. Res.*, this issue.

Schon, J., *Petrophysik*, p. 112, F. Enke, Stuttgart, Federal Republic of Germany, 1983.

Sisson, V. B., and T. C. Onstott, Dating blueschist metamorphism: A combined $^{49}Ar/^{39}Ar$ and electron microprobe approach, *Geochim. Cosmochim. Acta, 50*, 2111-2117, 1986.

Stewart, D. B., J. D. Unger, J. D. Phillips, R. Goldsmith, W. H. Poole, C. P. Spencer, A. G. Green, M. C. Loiselle, and P. St.-Julian, The Quebec–western Maine seismic reflection profile: Setting and first year results, in *Reflection Seismology: The Continental Crust, Geodyn. Ser.*, vol. 14, edited by M. Barazangi and L. Brown, pp. 189–199, AGU, Washington, D. C., 1986.

Winkler, G. R., and G. Plafker, Geological map and cross sections of the Cordova and Middleton Island quadrangles, southern Alaska, scale 1:250,000, *U.S. Geol. Surv. Open File Rep., 81-1164*, 25 pp., 1 sheet, 1981.

Winkler, G. R., M. L. Silberman, A Grantz, R. J. Miller, and E. M. MacKevett, Jr., Geological map and summary geochronology of the Valdez quadrangle, southern Alaska, scale 1:250,000, *U.S. Geol. Surv. Open File Rep., 80-892A*, 2 sheets, 1981.

T. M. Brocher, M. A. Fisher, and E. L. Geist, U.S. Geological Survey, 345 Middlefield Road, MS 977, Menlo Park, CA 94025.

N. I. Christensen, Department of Geosciences, Purdue University, West Lafayette, IN 47907.

(Received November 23, 1987;
revised February 16, 1988;
accepted February 17, 1988.)